



The pharmacokinetics and metabolism of diclofenac in chimeric humanized and murinized FRG mice

C. E. Wilson¹ · A. P. Dickie² · K. Schreiter³ · R. Wehr³ · E. M. Wilson⁴ · J. Bial⁴ · N. Scheer⁵ · I. D. Wilson⁶ · R. J. Riley⁷

Received: 2 February 2018 / Accepted: 25 April 2018
© Springer-Verlag GmbH Germany, part of Springer Nature 2018

Abstract

The pharmacokinetics of diclofenac were investigated following single oral doses of 10 mg/kg to chimeric liver humanized and murinized FRG and C57BL/6 mice. In addition, the metabolism and excretion were investigated in chimeric liver humanized and murinized FRG mice. Diclofenac reached maximum blood concentrations of 2.43 ± 0.9 $\mu\text{g/mL}$ ($n = 3$) at 0.25 h post-dose with an AUC_{inf} of 3.67 $\mu\text{g h/mL}$ and an effective half-life of 0.86 h ($n = 2$). In the murinized animals, maximum blood concentrations were determined as 3.86 ± 2.31 $\mu\text{g/mL}$ at 0.25 h post-dose with an AUC_{inf} of 4.94 ± 2.93 $\mu\text{g h/mL}$ and a half-life of 0.52 ± 0.03 h ($n = 3$). In C57BL/6J mice, mean peak blood concentrations of 2.31 ± 0.53 $\mu\text{g/mL}$ were seen 0.25 h post-dose with a mean AUC_{inf} of 2.10 ± 0.49 $\mu\text{g h/mL}$ and a half-life of 0.51 ± 0.49 h ($n = 3$). Analysis of blood indicated only trace quantities of drug-related material in chimeric humanized and murinized FRG mice. Metabolic profiling of urine, bile and faecal extracts revealed a complex pattern of metabolites for both humanized and murinized animals with, in addition to unchanged parent drug, a variety of hydroxylated and conjugated metabolites detected. The profiles in humanized mice were different to those of both murinized and wild-type animals, e.g., a higher proportion of the dose was detected in the form of acyl glucuronide metabolites and much reduced amounts as taurine conjugates. Comparison of the metabolic profiles obtained from the present study with previously published data from C57BL/6J mice and humans revealed a greater, though not complete, match between chimeric humanized mice and humans, such that the liver humanized FRG model may represent a model for assessing the biotransformation of such compounds in humans.

Keywords Liver · Humanized mice · Metabolism · Pharmacokinetics · Reactive metabolites

Electronic supplementary material The online version of this article (<https://doi.org/10.1007/s00204-018-2212-1>) contains supplementary material, which is available to authorized users.

✉ C. E. Wilson
claire.wilson@galderma.com

- ¹ Nestlé Skin Health R&D, Les Templiers, Route des Colles, BP 87, 06902 Sophia-Antipolis, France
- ² Evotec (UK) Ltd, 114 Innovation Drive, Abingdon, Oxfordshire OX14 4RZ, UK
- ³ Evotec International GmbH, Manfred Eigen Campus, Essener Bogen 7, Hamburg, Germany
- ⁴ Yecuris Corporation, PO Box 4645, Tualatin, OR 97062, USA
- ⁵ CEVEC Pharmaceuticals GmbH, Gottfried-Hagen-Str. 60-62, 51105 Cologne, Germany
- ⁶ Department of Surgery and Cancer, Imperial College, Exhibition Rd, South Kensington, London SW7 2AZ, UK
- ⁷ Evotec (UK) Ltd, Alderley Park, Nether Alderley, Cheshire SK10 4TG, UK

Introduction

Despite its relatively infrequent occurrence, drug-induced liver injury (DILI) is the leading cause of acute liver injury in the US (Kola and Lanhis 2004; Waring et al. 2015). Although much of the DILI observed is due to acetaminophen overdose, nonsteroidal anti-inflammatory drugs (NSAIDs), estimated to be used by more than 1% of the US population on a daily basis (Lichtenstein et al. 1995), are also seen as a common cause of hepatotoxicity. Hepatocellular injury is the most common pattern seen with NSAID hepatotoxicity and diclofenac (DCF) is the most frequently implicated agent (Schmeltzer et al. 2016). Serious liver injury has been reported to occur in 6.3 per 100,000 DCF users (de Abajo et al. 2004). DCF was introduced in the UK in 1979 and, despite the potential for DILI, is available without prescription as a generic drug in a number of formulations.

There are several metabolic pathways which have been implicated in DCF-related DILI in man, chiefly reactive quinone-imine intermediates generated via CYP450 metabolism (predominantly CYP2C) that can form adducts with cellular macromolecules unless detoxified via reaction with glutathione (Tang et al. 1999; Zhou et al. 2009). Alternatively, conjugation of the carboxylic acid moiety of DCF (and its metabolites) to form acyl glucuronides (DCF-AG) results in a metabolite which can form protein adducts by a variety of mechanisms (Boelsterli 2003), and it has been suggested that this can also cause toxicity. The underlying mechanisms and the determinants of susceptibility to DCF-induced DILI remain poorly defined. One proposed mechanism, in addition to simple damage caused by reaction with cellular macromolecules, is the hapten hypothesis (Park et al. 1987), a widely accepted theory to explain DILI that suggests that these adverse drug reactions are mediated by an adaptive immune response (Utrecht 2003). Autoantibodies have been detected both in patients who developed DILI after exposure to DCF and those who did not (Aithal et al. 2004). Experimental support for the hapten hypothesis is incomplete, and an animal model of liver injury and the involvement of antibodies or sensitized T cells (i.e., an adaptive immune response) has not emerged so far (Shaw et al. 2010). There is also evidence linking DCF with impaired mitochondrial function or induced mitochondrial permeabilization (Boelsterli and Lim 2007; Petrescu and Tarba 1997; Bort et al. 1999; Masubuchi et al. 2002; Gomez-Lechon et al. 2003a, b; Lim et al. 2006). However, it is important to note that mitochondrial dysfunction can be induced by a number of independent factors such as concurrent xenobiotic exposure, hypoxia, or inflammation (Shaw et al. 2010). Genetic polymorphisms in pro- or anti-inflammatory cytokines or in anti-apoptotic proteins could also render individuals more susceptible to DILI involving DCF, where patients who developed hepatotoxicity were more likely to have polymorphisms in IL-10 or IL-4 expression (Aithal et al. 2004). Furthermore, genetic polymorphisms in drug metabolizing enzymes (CYP2C8, UGT2B7, GST), and hepato-canalicular transporters (MRP2, MRP4) have been shown to play a role in the metabolism and disposition of DCF (Daly et al. 2007; Martinez et al. 2007; Reid et al. 2003). More recent results support the fact that several hepatic and renal transporters may play an important role in the distribution and elimination of DCF-AG (Zhang et al. 2016) and multifactorial pathways by which DCF-AG can act as a direct contributor to toxicity following DCF administration have been proposed (Scialis and Manautou 2016).

DILI remains a major clinical problem and poses considerable challenges and associated costs for drug development. Although the incidence for a particular drug may be very low, the outcome of DILI can be serious. Unfortunately, prediction has remained poor (both for patients at risk and

for new chemical entities) (Boelsterli and Lim 2007). Chimeric liver humanized mouse models, where human hepatocytes have been reported to replace > 90% of the murine hepatocytes, have been shown to have a value for various applications in drug metabolism and toxicity (Kamimura et al. 2010; Strom et al. 2010; Scheer and Wilson 2016). Our hypothesis for undertaking the studies described here is that the metabolism of DCF by chimeric humanized and murinized FRG mice would show a similar pattern to that observed *in vivo* in human and mouse, respectively, and could, therefore, be of use as a model to study DCF-related human DILI. To assess this hypothesis, the metabolite profiles of DCF in chimeric humanized and murinized FRG mice were compared with those previously described for normal C57BL/6J mice (Sarda et al. 2012, 2014) and the published data for humans (Willis et al. 1976; Riess et al. 1978; Stierlin et al. 1979; Stierlin and Faigle 1979; Faigle et al. 1988; Degen et al. 1988; Poon et al. 2001; Zhang et al. 2016).

Materials and methods

Chemicals

Diclofenac was purchased from Selleck Chemicals LLC (supplied by Absource Diagnostics GmbH, Munich, Germany) and used as supplied. Diclofenac acyl glucuronide standard was synthesized in house at AstraZeneca (Alderley Park, UK). 4'-hydroxydiclofenac and 5-hydroxydiclofenac were purchased from Santa Cruz Biotechnology Inc. (Dallas, Texas, USA) and 2-(2-nitro-4-trifluoro-methylbenzoyl)1,3-cyclohexedione (NTBC) was supplied by Yecuris (Tualatin, OR, USA). Tolbutamide, ammonium acetate and formic acid were purchased from Sigma-Aldrich (Dorset, UK) and leucine enkephalin was supplied by Waters Ltd (Elstree, UK). Analytical grade acetonitrile containing 0.1% formic acid, along with unmodified acetonitrile and methanol, was supplied by Fisher Scientific UK Ltd (Loughborough, UK).

Animal studies

All animal procedures were performed in accordance with Annex III of the Directive 2010/63/EU applying to national specific regulations as specified in the German law on animal protection. The PK of DCF in C57BL/6J mice was investigated in three male mice, 8 weeks of age, supplied by Charles River Laboratories (Sulzfeld, Germany). The PK and the routes, rate of excretion and metabolic fate of DCF were investigated in seven male chimeric humanized mice (HuFRGTM) and seven male chimeric murinized mice (MuFRGTM) (30 g), (FRG KO/C57BL/6J) [Yecuris (Tualatin, OR, USA)]. Following receipt, the mice were group housed

in cages of up to 3 and maintained under a 12 h light/dark cycle with free access to food and water, and conditions where temperature and humidity were controlled. The Hu-FRGTM and Mu-FRGTM animals were initially maintained on NTBC for 7 days, then removed from NTBC for 4 weeks prior to the first dose, according to the Yecuris protocol. Before commencing the study, a blood sample (25 μ L) was taken via the tail vein from each of the humanized mice to assess the human serum albumin (HSA) concentrations, and to ensure that the humanization of the liver was at least ca. 90% according to the Yecuris protocol. Animals were randomized according to body weight, and extent of humanization and then allocated to dosing groups. Groups of two Hu-FRGTM and Mu-FRGTM mice received dose vehicle (water) whilst each of five Hu-FRGTM and Mu-FRGTM and three C57BL/6J mice were administered DCF, at a nominal dose of 10 mg/kg, as a solution in water by oral gavage. Three animals from the Hu-FRGTM, Mu-FRGTM and C57BL/6J groups were taken for the determination of the PK of DCF. Whole blood (20 μ L) was collected pre-dose, and 0.25, 0.5, 1, 2, 4, 6 and 8 h post-dose from the tail vein into Minivette POCT K-EDTA-coated capillaries and then transferred to 96-well plates, pre-prepared with 20 μ L purified water containing 0.2% v/v phosphoric acid (to prevent the hydrolysis/rearrangement of acyl glucuronides), as soon as possible after collection. Gall bladders were taken from this PK group upon sacrifice at 8 h post-dose. The remaining two animals from the Hu-FRGTM and Mu-FRGTM groups were used to investigate the metabolite profile of DCF. The animals were placed individually in metabolic cages. Urine and faeces for metabolite profiling from animals dosed with DCF were collected, over dry ice to ensure sample stability, over 0–8 h and 8–24 h time periods. Urine and faeces from animals dosed with vehicle were collected over dry ice over a 24-h period, and used as controls for metabolite identification. Samples were frozen as soon as possible after collection on dry ice and stored at -80 °C until analysis. After the final sampling time point (8 h post-dose for the PK group, 24 h post-dose for the metabolite profiling group), the animals were anaesthetized by isoflurane inhalation and sacrificed by exsanguination. One aliquot, of up to 500 μ L, of Li-Heparin-plasma was obtained from the terminal bleed (in addition to the microsampling probe). The gall bladder was removed and stored at -80 °C until analysis.

Determination of humanization by ELISA

The level of humanization of each Hu-FRGTM mouse was estimated by measuring human albumin in mouse plasma using ELISA (Serum Albumin Human, Abcam # ab179887) according to the manufacturer's protocol. The same assay was performed on terminal plasma samples to assess

continuance of liver humanization during the study. The results are available in the supplementary data (Table S1).

Quantitative analysis of diclofenac in blood

Sample preparation

Aliquots of diluted blood (40 μ L) and diluted control blood spiked with DCF to provide calibration (30, 100, 300, 1000, 3000, 10,000 ng/mL) and QC samples (40, 400, 4000 ng/mL), were extracted by the addition of five volumes (v/v) of cold acidified acetonitrile (ACN) containing 200 nM tolbutamide as an internal analysis standard, mixed vigorously and centrifuged (4566g, 20 min) and diluted 1:2 (v/v) with water.

Sample analysis

Analysis of DCF in blood was performed by UHPLC–MS/MS using reversed-phase chromatography with a rapid gradient (1.3 min) on a BEH C18 column (Waters Ltd, Elstree, UK). Mass spectrometric analyses were conducted on an API 6500 triple quadrupole instrument (AB Sciex UK Ltd, Warrington, UK) operating in negative ion electrospray ionization (ESI) and multiple reaction monitoring modes (optimized transition for DCF was 294 > 250, with declustering potential DP -8 V, entrance potential EP -10 V, collision energy CE -15 V, and collision exit potential CXP -20 V). Non-optimized transitions corresponding to expected metabolites of DCF were also analyzed simultaneously. The instrument was controlled, and data acquired and processed by AnalystTM v.1.6.2 (AB Sciex UK Ltd, Warrington, UK). Instrument performance (chromatography and response of standards) was assessed before and after sample batch injection to ensure system suitability.

Blood pharmacokinetics

Phoenix WinNonlin 6.4 (Pharsight, Mountain View, CA) was used to generate PK parameter estimates using non-compartmental analysis. Peak (observed) blood concentrations (C_{max}) and AUC_{inf} , as determined by the linear trapezoidal rule were determined per animal and presented as the mean ($n=3$ for C57BL/6J mice, $n=3$ for Mu-FRGTM mice). For Hu-FRGTM mice, one mouse was terminated 4 h after dosing, so AUC_{inf} and $t_{1/2}$ are reported as the average of $n=2$.

Metabolite profiling and identification

Sample preparation

In addition to PK analysis, metabolite profiles were determined using aliquots of diluted blood (40 μ L) obtained from

animals pre-dose and 1, 2 and 4 h post-dose. Samples were extracted by the addition of four volumes (v/v) of ACN, with vigorous mixing, and centrifugation (4566g, 20 min) followed by dilution with 1:1 (v/v) with water. Urine samples obtained for metabolite profiling were pooled by dose group according to weight of urine collected, for each time range (0–8 h and 8–24 h for dosed animals, 0–24 h for vehicle animals). Pooled urine samples were centrifuged (20,800g, 5 min) to remove particulates. Gall bladders, removed at 8 h and 24 h, from dosed animals were extracted with eight volumes (w/v) of ACN, mixed vigorously, and sonicated for 30 min. The supernatants were pooled by dose group according to weight of gall bladder, centrifuged (20,800g, 5 min) to remove particulates and diluted 1:1 (v/v) with water.

Faeces samples were extracted twice with three volumes (w/v) of MeOH:H₂O 1:1 (v/v) and then with three volumes (w/v) of MeOH [with centrifugation (4566g, 20 min) after each extraction and removal of the supernatant]. Aliquots of the combined supernatants from each sample (0–8 and 8–24 h for dosed animals, 0–24 h for vehicle only mice) were pooled by dose group according to the weight of faeces collected and then evaporated from ca. 1 to ca. 200 μ L under a stream of dry nitrogen at ambient temperature.

Sample analysis

Metabolite profiles and identities were obtained using a reversed-phase gradient HPLC–QTOF–MS/MS method that had been developed previously to resolve DCF and its murine metabolites (Sarda et al. 2012). Briefly, 50 μ L aliquots of samples were separated on a Hypersil Gold C18 column (Fisher Scientific UK Ltd, Loughborough, UK) with a SecurityGuard C18, 3- μ m precolumn filtre (Phenomenex Inc., Macclesfield, UK) and eluted over 60 min. The post-column eluent was monitored by both a photodiode array detector (Waters Ltd, Elstree, UK) (210,400 nm at 20 spectra/s) and a Xevo G2 Q-ToF mass spectrometer (Waters Ltd, Wilmslow, UK) operated in positive ion ESI mode. The capillary voltage was set to +500 V, sampling cone to 25 V and extraction cone to 4 V. The source temperature was set to 150 °C, desolvation temperature to 500 °C, the cone gas flow was set to 50 L/h, and the desolvation gas flow to 1000 L/h. Mass spectrometric data were collected in resolution mode, in centroid data format, with a scan time of 1 s and a scan range of 50–1200 Th at a nominal resolution of 30,000. Full scan and product ion mass spectra were acquired simultaneously by HPLC–QTOF–MS^E. Collision energy was applied over a ramp of 20–40 eV for each product ion scan. The instrument was controlled and data acquired by MassLynxTM v.4.1 (Waters Ltd, Wilmslow, UK). Full scan and product ion mass spectra were interrogated by extracting chromatograms of potential metabolites using MassLynxTM v.4.1 from the raw data. Representative extracted ion spectra of DCF

and its metabolites are available in the supplementary data (Fig. S1). Comparison was also made with samples from the appropriate control group (or taken pre-dose) to minimize the potential for false positives from endogenous compounds. The mass spectrometer was calibrated with sodium formate (5 mM) in positive ion mode, and further aligned using an internal lock mass of 2 ng/mL leucine-enkephalin ([M + H]⁺ 556.2771 Th) infused at 10 μ L/min and scanned for 1 s every 57 s. Instrument performance (chromatography, response and mass accuracy of standards) was assessed before and after sample batch injection to ensure data quality. The measured mass accuracy for standards was less than 5 ppm.

Results

Clinical signs and degree of humanization

Plasma HSA concentrations were measured at >4 mg/mL in the humanized mice, consistent with the animals being >90% humanized on days 24 and 29 after removal of NTBC diet. One animal in the Hu-FRGTM mouse group was terminated 4 h after DCF dosing. There were no other clinical observations with all animals behaving normally following oral administration of either vehicle or DCF at 10 mg/kg.

Pharmacokinetics of diclofenac

The blood concentration versus time profiles for DCF in the Hu-FRGTM, Mu-FRGTM and C57BL/6J mice are shown in Fig. 1. After administration of the single oral dose (10 mg/kg) of DCF to Hu-FRGTM mice, the drug was rapidly absorbed, with mean peak blood concentrations of 2.43 ± 0.92 μ g/mL being reached at approximately 0.25 h post-dose. Good, but variable, exposure was achieved with the mean AUC_{inf} determined as 3.67 μ g h/mL ($n=2$) and a mean effective half-life of 0.86 h ($n=2$): profiles were indicative of enterohepatic recycling. Similarly following oral dosing of DCF to Mu-FRGTM mice rapid absorption was also seen, with mean peak blood concentrations of 3.86 ± 2.31 μ g/mL being reached at approximately 0.25 h post-dose. Similar exposure to that seen for the Hu-FRGTM mice was achieved with the mean AUC_{inf} for DCF determined as 4.94 ± 2.93 μ g h/mL and a mean half-life of 0.52 ± 0.03 h ($n=3$). Evidence of enterohepatic recycling was observed in only one Mu-FRGTM animal.

Following oral dosing of DCF to wild-type C57BL/6J mice ($n=3$) mean peak observed blood concentrations of 2.31 ± 0.53 μ g/mL were reached at approximately 0.25 h post-dose. Compared to the Mu-FRGTM mice, exposure of the C57BL/6J mice was less than twofold, with the mean AUC_{inf} determined as 2.10 ± 0.49 μ g h/mL and a mean

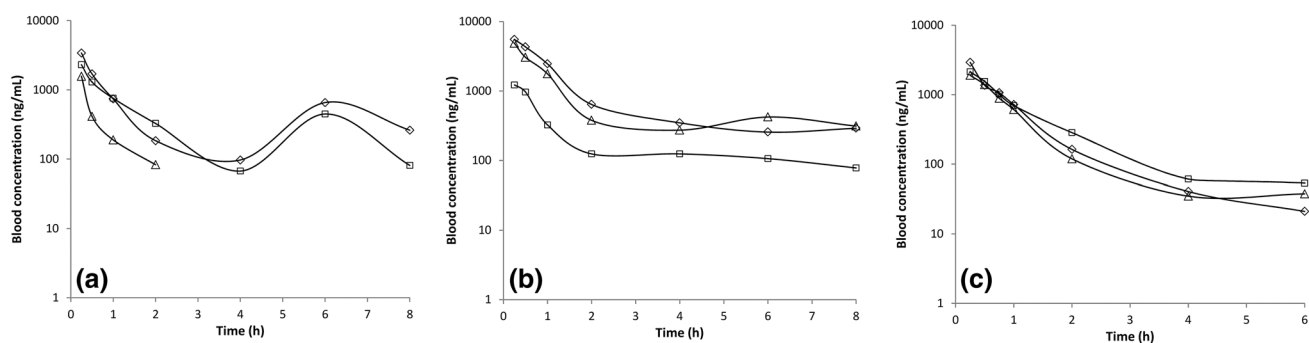


Fig. 1 Blood concentration–time profiles for diclofenac following single oral administration at 10 mg/kg to (a) Hu-FRGTM mice ($n=3$), (b) to Mu-FRGTM mice ($n=3$) and (c) C57BL/6J mice ($n=3$). Symbols represent concentration–time profiles from individual animals

half-life of 0.51 ± 0.49 h ($n=3$). No evidence of enterohepatic recycling was observed. By way of comparison of healthy male ($n=6$) and female human volunteers ($n=7$), when DCF was administered as a single 50 mg dose, peak plasma concentrations were achieved at 2.5 ± 1.1 and 1.25 ± 0.58 h post-dose in female and male subjects, respectively (Willis et al. 1976; Zhang et al. 2016). An apparent mean terminal half-life for DCF of 1.8 ± 2.1 h was observed in female subjects (Willis et al. 1976) but no data were presented for male subjects. The PK properties of DCF in Hu-FRGTM, Mu-FRGTM, wild-type C57BL/6J mice, and in healthy male and female subjects are compared in Table 1. Enterohepatic recycling was not observable in the human PK profiles (data not shown).

Diclofenac in blood

Only trace quantities of drug-related material were detected in the blood of animals at 24-h post-dose. Thus, DCF itself and the DCF-AG conjugate (M44) were detected in the

blood of both Hu-FRGTM and Mu-FRGTM mice whilst the taurine conjugate (M48) was only observed in the blood of Mu-FRGTM mice.

Diclofenac and metabolites in urine

The LC–MS profiles observed for the 0–8 h (data not shown) and 8–24 h urine samples (Fig. 2a) were similar for Hu-FRGTM mice. The same observation was made for the Mu-FRGTM mice (Fig. 2b). The chromatographic and mass spectrometric properties of these metabolites are provided in Table 2. A full summary table of HPLC and mass spectrometric data obtained for DCF and its metabolites in both Hu-FRGTM and Mu-FRGTM mouse urine, faeces, bile and blood is provided in the supplementary data (Table S2). In the absence of authentic standards, it was not possible to quantify the amounts of each metabolite produced and, as a result only a qualitative comparison between Hu-FRGTM and Mu-FRGTM mice could be reported.

Table 1 Pharmacokinetic parameters for diclofenac in C57BL/6J mice, Mu-FRGTM mice, HuFRGTM mice, and in healthy human male and female subjects

	Blood Hu-FRG TM mice	Blood Mu-FRG TM mice	Blood C57BL/6J mice	Plasma healthy female subjects ^a	Plasma healthy male subjects ^b
Dose (mg/kg)	10	10	10	0.80	0.71
C_{\max} ($\mu\text{g/mL}$)	2.43 ± 0.92	3.86 ± 2.31	2.31 ± 0.53	2.0 ± 0.7	0.91 ± 0.16
T_{\max} (h)	0.25	0.25	0.25	2.5 ± 1.1	1.25 ± 0.58
AUC_{inf} ($\mu\text{g h/mL}$)	3.67^c	4.94 ± 2.93	2.10 ± 0.49	1.67 ± 0.44	1.20 ± 0.19
$t_{1/2}$ (h)	$0.86^{c,d}$	0.52 ± 0.03	0.51 ± 0.49	1.8 ± 2.1	ND

Values are mean \pm SD unless otherwise stated

^aData taken from Willis et al. 1976. Seven subjects received a single 50 mg oral dose of diclofenac sodium (enteric-coated tablet). Using the mean weight of the subjects (62.3 ± 8.4 kg), the dose can be calculated as 0.80 mg/kg

^bData taken from Zhang et al. 2016. Six subjects received a single-dose administration of 50 mg of Voltafam (diclofenac potassium, Novartis (India) Ltd., Mumbai, India). Using a nominal weight of 70 kg, the dose can be calculated as 0.71 mg/kg. ND, no data were provided for the $t_{1/2}$

^cCalculated using $n=2$ mice (one mouse was terminated 4 h after dosing)

^dEffective half-life was calculated due to evidence of enterohepatic recycling

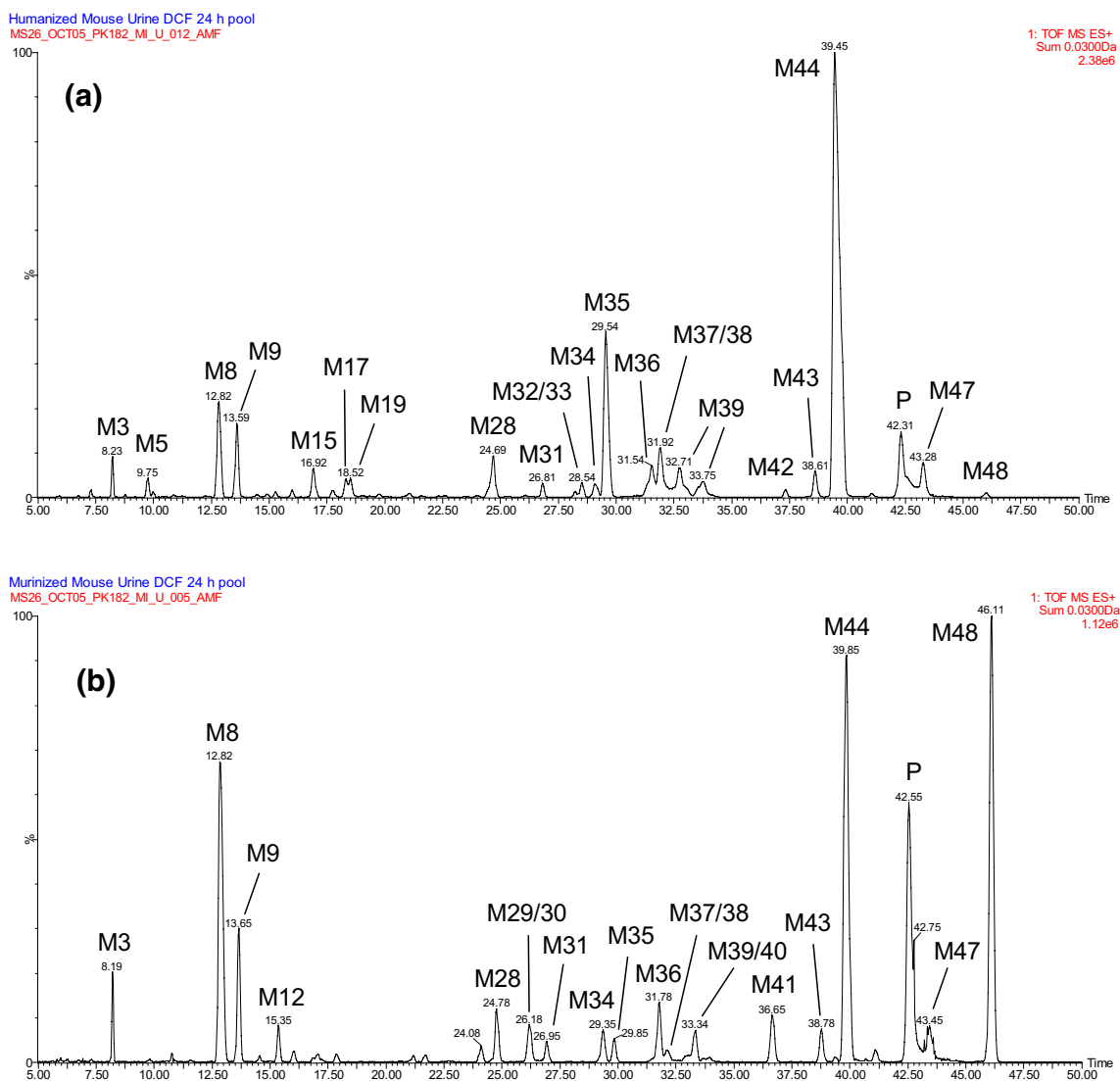


Fig. 2 LC–QTOF–MS profiles of diclofenac and its most abundant metabolites in urine 8–24 h following single oral administration of 10 mg/kg diclofenac to **a** Hu-FRGTM mice and **b** Mu-FRGTM mice

Extensive metabolism was observed in Hu-FRGTM mice (Fig. 2a), dominated by the signal for the DCF-AG conjugate (M44), and hydroxy-glucuronide (M35) accompanied by smaller amounts of minor transacylated glucuronides (M47). Unchanged DCF was also detected (possibly in part derived from hydrolysis of DCF-AG conjugates) whilst the LC–MS profiles also showed a large number of less intense signals corresponding to a range of hydroxylated, lactamized and glucuronidated metabolites with small amounts of taurine conjugates, hydroxymethyl metabolites (M7 and M11) and a riboside (M18) also present.

Extensive metabolism also occurred in Mu-FRGTM mice (Fig. 2b), dominated by the signal for the DCF-AG conjugate (M44), accompanied by large amounts of direct taurine conjugates (M48). Unchanged DCF was also detected

(again potentially in part derived from hydrolysis of acyl glucuronide conjugates) whilst the LC–MS profiles also showed, as seen with the Hu-FRGTM mice, a range of less intense signals for various hydroxylated metabolites. For C57BL/6J mice (Sarda et al. 2012), the relative signals for the hydroxyglucuronide (M3) and taurine (M48) metabolites appeared more intense compared to those seen for Mu-FRGTM mice in the present study (Table 4). A hydroxy-ribose conjugate (M18) was observed in the urine of Hu-FRGTM, Mu-FRGTM and C57BL/6J mice (Tables 2, 4). This metabolite corresponds to the putative hydroxy-riboside (denoted M15) observed in C57BL/6J mice following a single oral dose of [¹⁴C]-DCF at 10 mg/kg previously reported as a novel conjugation by Sarda et al. (2012) following analysis of urine and faeces. In

Table 2 Summary of HPLC and mass spectrometric data obtained for diclofenac and selected (major and differentiating) metabolites detected in Hu-FRGTM and Mu-FRGTM mouse urine, faeces, bile and blood

Peak ID	<i>t_R</i> (min)	Assignment	Elemental composition [M + H] ⁺	Theoretical <i>m/z</i> (³⁵ Cl/ ¹² C isotope [M + H] ⁺)	Δ <i>m</i> [observed-theoretical <i>m/z</i>] (mDa) Hu-FRG TM	Δ <i>m</i> [observed-theoretical <i>m/z</i>] (mDa) Mu-FRG TM	Presence in biofluids
P	42.4	Diclofenac	C14H12Cl2N1O2	296.0240	+0.1	0.0	U, B, F, P
M2	7.3	Dihydroxy	C14H12Cl2N1O4	328.0138	+0.8	ND	U, B
M3	8.2	Hydroxy glucuronide	C20H20Cl2N1O9	488.0510	+0.9	-0.3	U, B
M5	9.8	Hydroxy glucuronide	C20H20Cl2N1O9	488.0510	+0.6	-	U, B
M7	11.4	Hydroxy-methoxy	C15H14Cl2N1O4	342.0294	-1.3	-	U
M8	13.0	Hydroxy glucuronide	C20H20Cl2N1O9	488.0510	+0.2	-0.4	U, B
M9	13.7	Hydroxy glucose	C20H22Cl2N1O8	474.0717	0.0	+0.8	U, B
M10	14.5	Hydroxy glucuronide	C20H20Cl2N1O9	488.0510	+1.3	-0.2	U
M11	15.0	Hydroxy-methoxy	C15H14Cl2N1O4	342.0294	-0.5	-	U
M12	15.4	Hydroxy mercapturate	C19H19Cl2N2O6S	473.0335	+0.5	+0.1	U, B
M13	16.1	Hydroxy glucuronide, indolinone	C20H18Cl2N1O8	470.0404	+0.3	0.0	U, B
M15	17.0	Dihydroxy	C14H12Cl2N1O4	328.0138	+0.2	+0.1	U, B
M16	17.9	Hydroxy	C14H12Cl2N1O3	312.0189	+0.3	+0.8	U
M17	18.4	Dihydroxy	C14H12Cl2N1O4	328.0138	+0.1	-	U
M18	18.4	Hydroxy ribose	C19H20Cl2N1O7	444.0611	+0.4	+0.2	U
M19	18.7	Hydroxy-deschloro, cysteine	C17H18Cl1N2O5S	397.0619	0.0	-	U, B
M21	19.9	Hydroxy-deschloro, cysteine	C17H18Cl1N2O5S	397.0619	+0.5	-	U
M24	22.4	Hydroxy glucuronide	C20H20Cl2N1O9	488.0510	+0.8	-	U
M25	22.6	Hydroxy glucuronide	C20H20Cl2N1O9	488.0510	+0.3	-	U
M26	23.2	Deschloro, cysteine	C17H18Cl2N2O4S	381.0670	-	-0.1	U
M27	24.6	Hydroxy glucuronide, indolinone	C20H18Cl2N1O8	470.0404	+0.2	+0.2	U
M28	24.8	Hydroxy glucuronide, indolinone (Na⁺)	C20H17Cl2N1O8Na	492.0223	0.0	+0.1	U
M29	26.2	Hydroxy cysteine	C17H17Cl2N2O5S	431.0230	+0.3	-0.5	U
M33	28.6	Hydroxy glucuronide (Na ⁺)	C20H19Cl2N1O9Na	510.0329	+0.3	-	U, B
M34	29.2	Hydroxy	C14H12Cl2N1O3	312.0189	+0.3	+0.4	U, B
M35	29.7	Hydroxy glucuronide (Na⁺)	C20H19Cl2N1O9Na	510.0329	-0.2	0.0	U, B, F
M36	31.7	Hydroxy	C14H12Cl2N1O3	312.0189	0.0	0.2	U, B
M37	32.0	Hydroxy	C14H12Cl2N1O3	312.0189	-0.2	0.0	U
M38	32.0	Acyl glucuronide	C20H20Cl2N1O8	472.0560	-0.5	+0.2	U

Table 2 (continued)

Peak ID	t_R (min)	Assignment	Elemental composition [M + H] ⁺	Theoretical m/z (³⁵ Cl/ ¹² C isotope [M + H] ⁺)	Δm [observed-theoretical m/z] (mDa) Hu-FRG TM	Δm [observed-theoretical m/z] (mDa) Mu-FRG TM	Presence in biofluids
M39	31.5–33.8	Transacylated hydroxy glucuronide (cluster)	C20H20Cl2N1O9	488.0510	0.0	– 0.1	U, B
M40	33.2	Hydroxy taurine	C16H17Cl2N2O5S	419.0230	+ 2.3	– 0.1	U, F
M41	36.6	Hydroxy taurine	C16H17Cl2N2O5S	419.0230	+ 1.1	– 0.2	U
M42	37.4	Unassigned conjugate	ND	470.0340	ND	-	U, B, F
M43	38.7	Acyl glucuronide (Na⁺)	C20H19Cl2N1O8Na	494.0380	+ 0.5	+ 0.4	U
M44	39.6	Acyl glucuronide (Na⁺)	C20H19Cl2N1O8Na	494.0380	+ 0.1	+ 1.0	U, B, P
M45	40.6	Acyl glucuronide	C20H20Cl2N1O8	472.0560	+ 0.2	+ 0.8	U
M47	42.4–43.3	Transacylated glucuronides (cluster)	C20H20Cl2N1O8	472.0560	+ 0.1	– 1.0	U, B
M48	46.0	Taurine	C16H17Cl2N2O4S	403.0281	– 0.1	– 0.2	U, B, F, P

Metabolites found in both humanized and murinized mice are in bold. Those found only in humanized mice are in normal font, and those found only in murinized mice are in italic font. The complete list of metabolites is available in the supplementary data (Table S2)

Metabolite detected in biofluid

U urine, B bile, F faeces, B blood, ND not determined

the present study, M18 was only found in urine and not faeces or bile.

Also detected in the urine of Hu-FRGTM mice were minor metabolites assigned as cysteine conjugates of hydroxy-deschloro intermediates (M19 and M21) which were not observed for either the Mu-FRGTM mice, or in the previous study in C57BL/6J animals. In the urine of Mu-FRGTM mice, a deschloro-cysteinyl metabolite (M26) was observed, whilst in samples from both Mu-FRGTM and Hu-FRGTM mice a hydroxyl-cysteinyl metabolite (M29) was detected. Glutathione-derived metabolites of this type were not reported by Sarda et al. (2012) in the urine of C57BL/6J mice.

Metabolite profiles of diclofenac in bile

The LC–MS profiles observed for the 8-h bile samples from both Hu-FRGTM and MuFRGTM mice (Fig. 3) showed the presence of a number of hydroxylated and conjugated metabolites of DCF. The biliary metabolite profile for the Hu-FRGTM mice was dominated by the ether glucuronide (M3, M5, M8) and hydroxyglucuronide (M35) conjugates, dihydroxy-DCF (M15) and an unassigned conjugate (M42), with the cysteine conjugate of a hydroxy-deschloro intermediate (M19) also present. Other metabolites included the lactamized indolinone forms of the hydroxyglucuronide conjugates (M27/28), hydroxyglucuronides (M32/33) and

hydroxy-DCF (M34). Unchanged DCF was also detected (possibly in part derived from hydrolysis of the DCF-AG).

The biliary profile of the Mu-FRGTM mice was dominated by hydroxy-glucuronide conjugates (M3, M8), the DCF-AG (M44) and taurine conjugates (M48). Other metabolites detected in bile included the hydroxy-mercaptopurinate (M12), hydroxyglucuronide indolinone (M27/28), hydroxy-DCF (M34) and hydroxyglucuronide (M35). Unchanged DCF was also detected (again, in part possibly resulting from the hydrolysis of the DCF-AG). In the bile samples obtained at 24 h post-dose, from both types of chimeric mice (metabolite profiles not shown), only the ether glucuronide conjugates (M3, M8) were detected and these were present only in trace quantities. Metabolite information is summarized in Table 2.

Metabolite profiles of diclofenac in faecal extracts

The LC–MS profiles observed for the faecal extract (8–24 h) from both male Hu-FRGTM and Mu-FRGTM mice (Fig. 4) showed small amounts of DCF present. In addition, extracts from the faeces of Hu-FRGTM mice contained hydroxy-DCF (M34) and an unassigned conjugate (M42) which were not present in Mu-FRGTM mice. Additionally, Mu-FRGTM mouse faecal extracts contained taurine (M48), hydroxy-aurine (M40, M41) and hydroxy-glucuronide (M24/25) metabolites

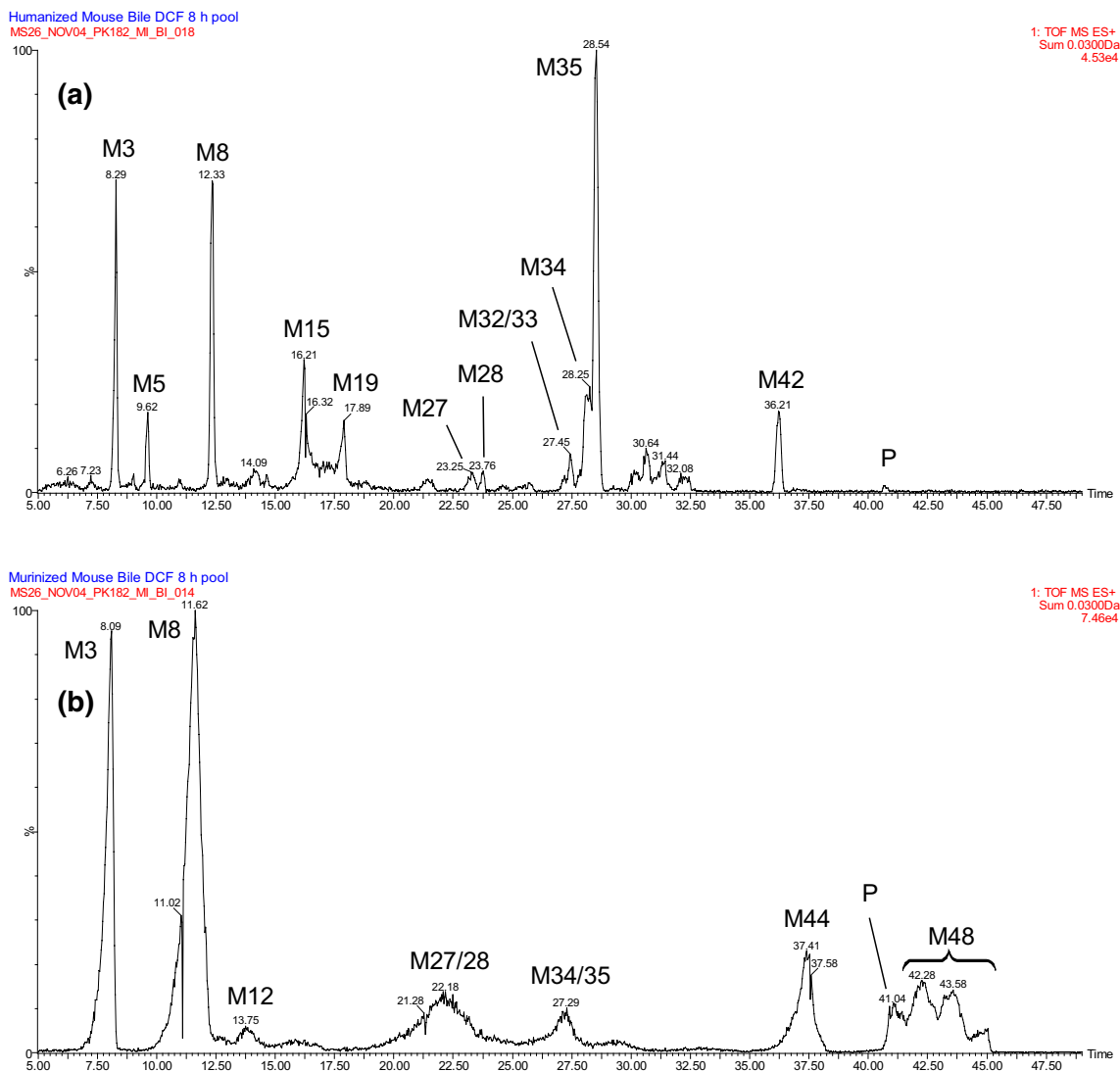


Fig. 3 LC-QTOF-MS profiles of diclofenac and its most abundant metabolites in bile 8 h following single oral administration of 10 mg/kg diclofenac to **a** Hu-FRGTM mice and **b** Mu-FRGTM mice. The Mu-

FRGTM bile sample suffered from poor chromatography. Due to limited sample volume the analysis could not be repeated

which were absent from the faecal extracts of the Hu-FRGTM mice.

Discussion

The present studies reveal the complexity of the metabolic fate of DCF in both Hu-FRGTM and Mu-FRGTM mice, involving a broad range of oxidative functionalization reactions and glucuronide, taurine and glutathione conjugations as summarized in Tables 2 and 3, and depicted in Figs. 2, 3, 4, 5 and 6. Some of these metabolites have already been reported as common to both humans and C57BL/6J mice and, as expected, the excreta of both the chimeric Hu-FRGTM and Mu-FRGTM mice shared a number

of metabolites (to facilitate comparison these metabolite profiles are summarized in a “heat”, or “met”, “map” in Table 4). In all three types of mouse model (wild type, Hu-FRGTM and Mu-FRGTM) and humans, the “universally” detected metabolites included hydroxy (M34, M36, M37), dihydroxy (M15), hydroxy-glucuronides (M3, M8, M35), AG (M44) and transacylated glucuronides of DCF (e.g., M47). However, it is also clear that the Mu-FRGTM mice, which had been repopulated with hepatocytes derived from C57BL/6J mice, whilst producing many of the same metabolites, were not (based on the results of Sarda et al. 2012, 2014) equivalent to the C57BL/6J animals but also produced some metabolites seen in the profiles of the Hu-FRGTM mice. Similar observations were made when comparing the metabolism of lumiracoxib in Hu-FRGTM,

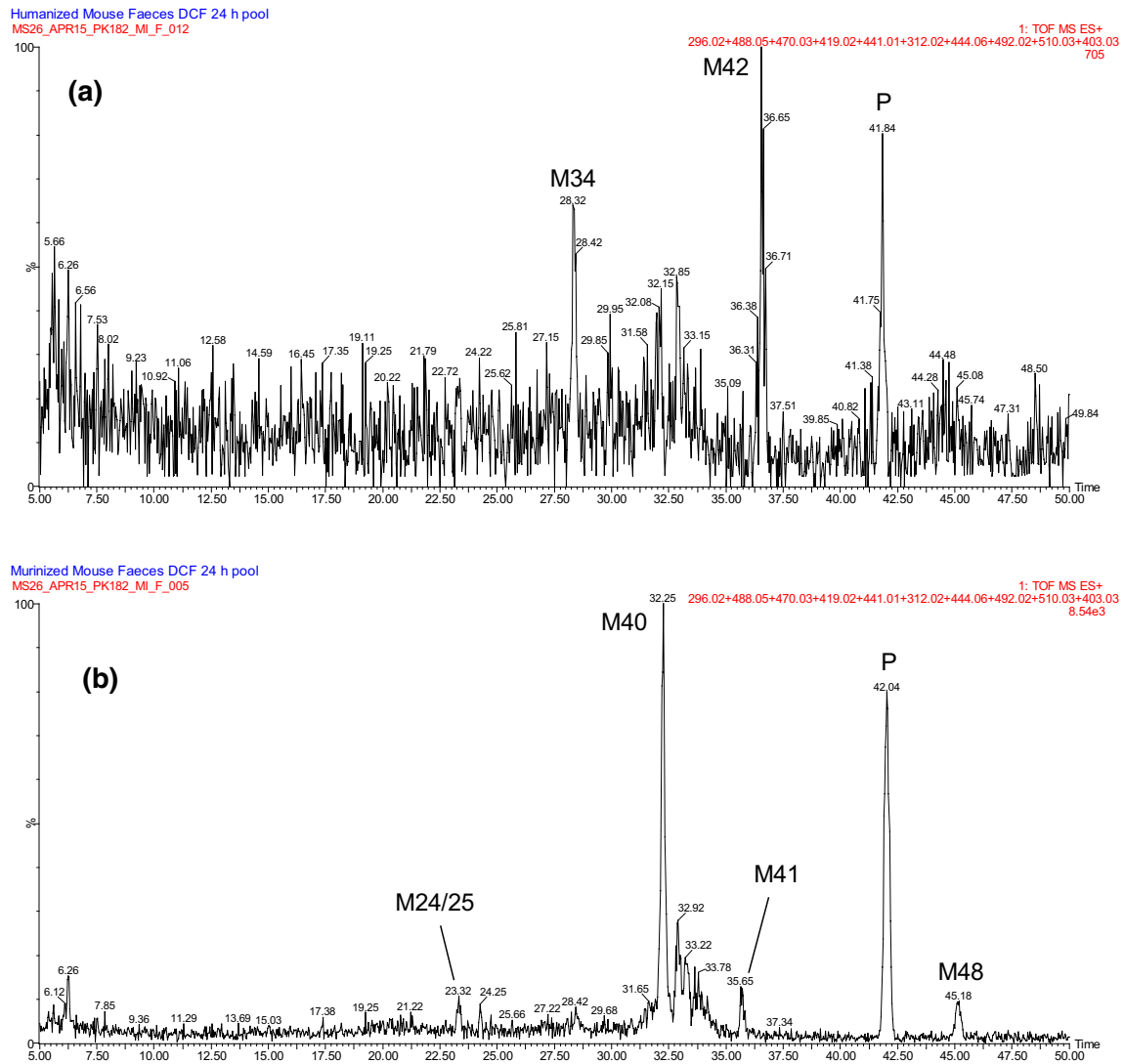


Fig. 4 LC–QTOF–MS profiles of diclofenac and its most abundant metabolites in faeces 8–24 h following single oral administration of 10 mg/kg diclofenac to **a** Hu-FRGTM mice and **b** Mu-FRGTM mice

Table 3 Summary of peak heights for direct taurine conjugates (M48) and hydroxytaurines (M40 and M41) detected in Hu-FRGTM and Mu-FRGTM mouse urine, faeces, bile and blood at 8 and 24 h after dosing

Peak heights	Taurine M48 46.0 min	OH Taurine M40 33.2 min	OH Taurine M41 36.6 min
Mu-FRG TM 8 h	9.97E+05	6.68E+04	7.53E+04
Mu-FRG TM 24 h	1.12E+06	6.77E+04	1.04E+05
Hu-FRG TM 8 h	1.40E+04	2.24E+03	1.15E+03
Hu-FRG TM 24 h	2.58E+04	3.40E+03	1.46E+03
Ratio 8 h Mu-FRG TM /Hu-FRG TM	71	30	65
Ratio 24 h Mu-FRG TM /Hu-FRG TM	43	20	71
Mean ratio Mu-FRG TM /Hu-FRG TM	57	25	68

Mu-FRGTM, C57BL/6J mice and humans (Dickie et al. 2017). Such a result may reflect either “strain” differences, gene expression changes in Mu-FRGTM mice compared

to wild-type animals, or perhaps extrahepatic “murine” metabolism in, e.g., the gut or kidney [although previous studies in hepatic reductase null (HRN) mice suggest that

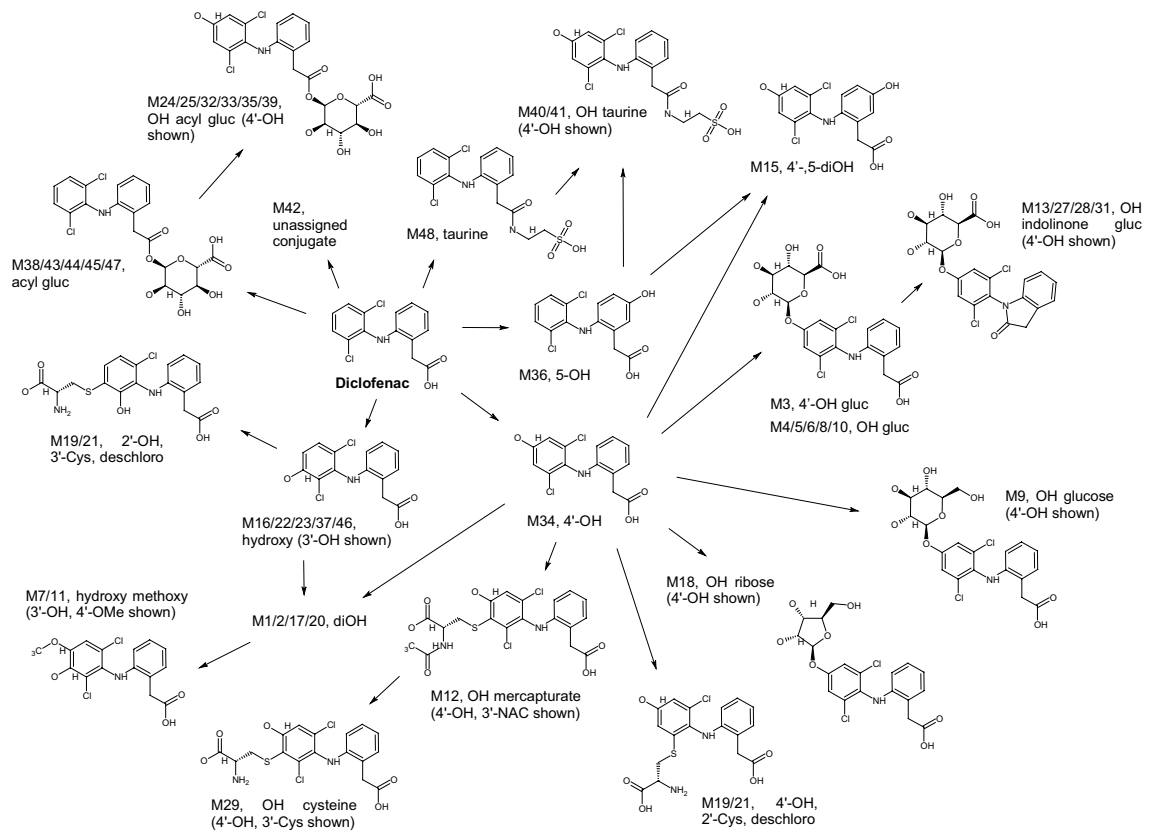


Fig. 5 Proposed metabolic fate of diclofenac in Hu-FRG™ mouse

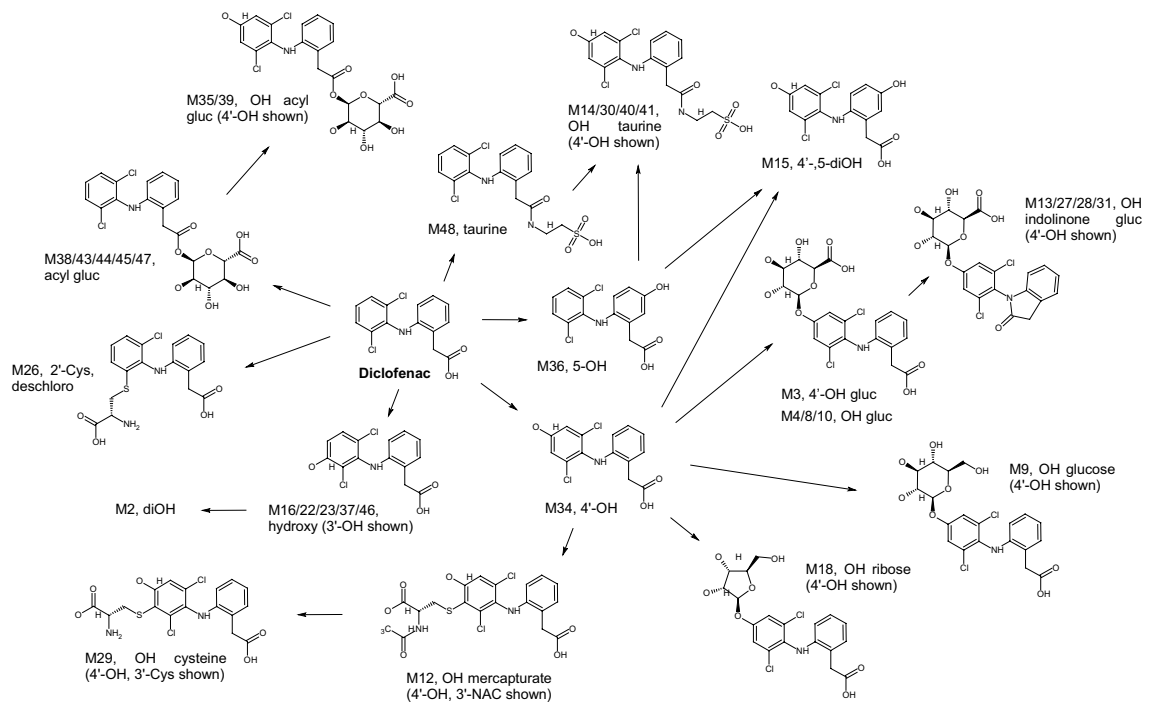


Fig. 6 Proposed metabolic fate of diclofenac in Mu-FRG™ mouse

Table 4 Comparison of diclofenac and selected (major and differentiating) metabolites observed in excreta from human ADME studies (and from a human in vitro study), the present study with Hu-FRGTM and Mu-FRGTM mice, and wild-type C57BL/6J mice

Peak ID	Assignment	Human	Hu-FRG TM	Mu-FRG TM	C57BL/6J ^{b,c}
P	Diclofenac	In vivo Stierlin and Faigle (1979)	+++	+++	++
M2	Dihydroxy		++	+	–
M3	Hydroxy glucuronide	In vitro Kumar et al. (2002)	+++	+++	++++
M5	Hydroxy glucuronide	In vitro Kumar et al. (2002)	++	–	–
M7	Hydroxy-methoxy	In vivo Faigle et al. (1988)	+	–	–
M8	Hydroxy glucuronide	In vitro Kumar et al. (2002)	+++	+++	+++
M9	Hydroxy glucose		++	+++	+++
M10	Hydroxy glucuronide	In vitro Kumar et al. (2002)	+	++	–
M11	Hydroxy-methoxy	In vivo Faigle et al. (1988)	++	–	–
M12	Hydroxy mercapturate	In vivo Poon et al. (2001)	++	++	–
M13	Hydroxy glucuronide, indolinone		++	++	–
M15	Dihydroxy	In vivo Stierlin and Faigle (1979)	+++	+	+
M16	Hydroxy	In vivo Stierlin and Faigle (1979)	++	+	–
M17	Dihydroxy		++	–	–
M18	Hydroxy ribose		+	+	+
M19	Hydroxy-deschloro, cysteine		++	–	–
M21	Hydroxy-deschloro, cysteine		++	–	–
M24	Hydroxy glucuronide		++	–	–
M25	Hydroxy glucuronide		++	–	–
M26	Deschloro, cysteine		–	+	–
M27	Hydroxy glucuronide, indolinone		++	+	–
M28	Hydroxy glucuronide, indolinone		+++	+++	+
M29	Hydroxy cysteine		+	++	–
M33	Hydroxy glucuronide		++	–	–
M34	Hydroxy	In vivo Stierlin and Faigle (1979)	+++	+	++
M35	Hydroxy glucuronide		+++	++	+
M36	Hydroxy	In vivo Stierlin and Faigle (1979)	+++	++	++ ^a
M37	Hydroxy	In vivo Stierlin and Faigle (1979)	+++	++	–
M38	Acyl glucuronide	In vitro Kumar et al. (2002)	+++	++	–
M39	Transacylated hydroxy glucuronide (cluster)		+++	+	+
M40	Hydroxy taurine		+	+	++
M41	Hydroxy taurine		+	++	++
M42	Unassigned conjugate		++	–	–
M43	Acyl glucuronide	In vitro Kumar et al. (2002)	+++	++	–
M44	Acyl glucuronide (Na+)	In vitro Kumar et al. (2002)	++++	++++	++ ^a
M45	Acyl glucuronide	In vitro Kumar et al. (2002)	+	++	–
M47	Transacylated glucuronides (cluster)	In vitro Kumar et al. (2002)	+++	++	+
M48	Taurine		+	+++	++++

++++ detected 5×10^5 ; +++ detected $> 10^5$; ++ detected $> 10^4$; + detected $> 10^3$, in the present study, or equivalent relative measures in the human and mouse studies; – not reported/below level of detection

^aSingle metabolite observed in a human or mouse study may correspond to one or more metabolites observed in the present study

^bSarda et al. (2012)

^cSarda et al. (2014)

hepatic metabolism predominates in the mouse (Pickup et al. 2012)].

Major metabolites in both Mu-FRGTM and C57BL/6J mice were the taurine conjugates (M40, M41 and M48),

which were also detected in much less amounts in the Hu-FRGTM mice (Table 4). In comparing taurine conjugation between Hu-FRGTM and Mu-FRGTM mice, the mean ratio was found to be above 57:1 in favour of the murinized mice

for the direct taurine conjugate, whilst for the hydroxy taurine metabolites the ratio was 25–68:1 in favour of the murinized mice (Table 3). Given the propensity for taurine conjugation in the mouse, the detection of taurine conjugates following administration of DCF to Hu-FRGTM mice may be due to the residual murine hepatocytes in the liver of these chimeric animals. This apparent “mouse-specific” production of taurine conjugates from carboxylic acid-containing drugs such as DCF and lumiracoxib (and their metabolites) (Dickie et al. 2017) may, therefore, represent a “biomarker” of the residual mouse-specific xenobiotic metabolism due to the remaining mouse hepatocytes present in the liver of the Hu-FRGTM mice.

In terms of pharmacokinetics, the exposure of DCF in C57BL/6J, Mu-FRGTM and Hu-FRGTM mice was similar. There was, however, evidence of enterohepatic recycling in the PK profiles for DCF in Hu-FRGTM mice (Fig. 1a) but not in the majority of the Mu-FRGTM mice (Fig. 1b) or C57BL/6J mice (Fig. 1c). Studies in humans [e.g., Schneider et al. (1990)] described the biliary excretion of small amounts (1–9%) of unchanged DCF.

In the present study, there was strong evidence for the formation of transacylated products (M38, M43, M45) from the 1- β -*O*-acyl glucuronide of DCF (M44) and this is consistent with previous work with C57BL/6J mice (Sarda et al. 2012, 2014). The detection of DCF-AG and related compounds may be significant in terms of the generation of reactive metabolites, given the ability of these acyl glucuronides to react with proteins (Kretz-Rommel and Boelsterli 1993, 1994; Hargus et al. 1994; Le and Franklin 1997; Boelsterli 2003). Indeed, a recent investigation (Hammond et al. 2014) has demonstrated the presence of a complex pattern of adducts to HSA in samples derived from patients, with various combinations of *N*-acylations and AG glycations characterized. The production of the DCF-AG is also significant for intestinal toxicity, as opposed to DILI, as hydrolysis back to the aglycone, catalyzed by bacterial glucuronidases produced by the gut microbiota, has been shown to cause DCF-induced enteropathy in mice (LoGuidice et al. 2012).

The metabolite profiles obtained from the Mu-FRGTM and Hu-FRGTM mice also revealed the presence of cysteinyl and *N*-acetylcysteinyl (mercapturate) metabolites, presumably the result of the further metabolism of glutathione conjugates, often associated with reactive metabolite-related toxicity. A number of these appear to have resulted from the metabolic dechlorination of DCF, with the pattern seemingly dependent on the nature of the hepatocytes used to repopulate the livers. Specifically, the hydroxy-deschloro-cysteinyl conjugates (M19 and M21) were only observed in Hu-FRGTM mice whilst the deschloro-cysteinyl conjugate (M26) was only detected in Mu-FRGTM mice [but not C57BL/6J mice (Sarda et al. 2012, 2014)]. The hydroxy-mercapturate conjugate (M12) was observed in urine and bile of both

Hu-FRGTM and Mu-FRGTM mice (but not C57BL/6J mice (Sarda et al. 2012, 2014)) and has previously been detected as a result of *in vitro* studies using human liver microsomes (Kumar et al. 2002). Similarly, the hydroxy-cysteine metabolite (M29) was observed in the urine of both Hu-FRGTM and Mu-FRGTM mice. The formation of these cysteinyl and mercapturate conjugates provides evidence for potential toxicity and was observed at different intensities in the present study in both Hu-FRGTM and Mu-FRGTM mice. The presence of mercapturate and cysteine conjugates (M12, M26 and M29) in Mu-FRGTM mice was surprising because although such metabolites have been observed in the urine of rats and humans treated with DCF (Poon et al. 2001), they were not detected in studies on C57BL/6J mice (Sarda et al. 2012).

The Hu-FRGTM mice produced a number of human-specific metabolites that had previously been found *in vitro* (Kumar et al. 2002), but which were less abundant in Mu-FRGTM, such as the hydroxy-glucuronides (M5, M24, M25, M33), cysteine conjugates (M19, M21), DCF-hydroxy glucuronide (M35) and an unassigned conjugate (M42). One minor metabolite, hydroxy-methoxy-DCF (M7 and M11) (Tables 2, 4) was observed in Hu-FRGTM urine and may correspond to “metabolite VI” (Faigle et al. 1988; Degen et al. 1988) which was found to accumulate in human plasma and was also observed in human urine, albeit only in small amounts (ca. 1% dose). The same metabolite was also observed in the plasma of chimeric, liver humanized, TK-NOG mice (Kamimura et al. 2010). In the present study, the presence of metabolites M7 and M11 only appeared in urine of Hu-FRGTM mice and were not observed in blood at this dose. Overall, there were nevertheless significant qualitative differences in the metabolite profiles between the various models, including evidence of unique metabolites for the Hu-FRGTM animals. The metabolic fate of DCF in Hu-FRGTM mice using LC-MS did, however, share some commonality with those of chimeric Mu-FRGTM and wild-type C57BL/6J mice (with the Mu-FRGTM profiles somewhat intermediate between the C57BL/6J and Hu-FRGTM mice).

Differences were also observed between the metabolism of DCF in Hu-FRGTM mice and that reported for studies in humans (see Table 4). Determining if these novel metabolites detected in the profiles obtained for the Hu-FRGTM accurately recapitulate human metabolism is complicated by the fact that the studies performed to understand the metabolism of DCF in humans were performed over 30 years ago. It is, therefore, perhaps unsurprising that a number of minor metabolites of DCF were detected in Hu-FRGTM mice that have not been reported for humans (Table 4). Moreover, some of the differences observed were associated with a range of novel and relatively minor compounds found in the present study in mice rather than the major known human metabolites. This suggests that the reinvestigation of the human *in vivo* biotransformation of DCF, using modern

techniques, might both improve our understanding of the human metabolism of the drug and, if these novel minor metabolites were shown to be present, validate further the predictive capabilities of the Hu-FRGTM mice. The characterisation of the biotransformation of DCF in humans using modern LC–MS-based technologies has, to date, not yet been undertaken.

With respect to the DILI, associated with DCF, both the acyl glucuronide and oxidative metabolic routes have been advanced as hypothetical mechanisms in the formation of reactive metabolites, and subsequent covalent binding to proteins detected in both in vitro or in vivo studies (Park et al. 1987; Tang et al. 1999; Boelsterli 2003; Uetrecht 2003; Aithal et al. 2004; Zhou et al. 2009; Shaw et al. 2010; Pickup et al. 2012; Hammond et al. 2014). The combination of much higher production of acyl glucuronides together with the detection of a “human-specific” pattern of glutathione-derived conjugates in the Hu-FRGTM mouse in this study suggests that this model may have some value in the investigation of in vivo mechanisms of DCF-related human DILI.

Compliance with ethical standards

Conflict of interest The authors declare that they have no conflict of interest.

References

- Aithal GP, Ramsay L, Daly AK, Sonchit N, Leathart JB, Alexander G, Kenna JG, Caldwell J, Day CP (2004) Hepatic adducts, circulating antibodies, and cytokine polymorphisms in patients with diclofenac hepatotoxicity. *Hepatology* 39:1430–1440
- Boelsterli UA (2003) Diclofenac-induced liver injury: a paradigm of idiosyncratic drug toxicity. *Toxicol Appl Pharmacol* 192:307322
- Boelsterli UA, Lim PL (2007) Mitochondrial abnormalities—a link to idiosyncratic drug hepatotoxicity? *Toxicol Appl Pharmacol* 220:92107
- Bort R, Ponsoda X, Jover R, Gómez-Lechón MJ, Castell JV (1999) Diclofenac toxicity to hepatocytes: a role for drug metabolism in cell toxicity. *J Pharmacol Exp Ther* 288(1):65–72
- Daly AK, Aithal GP, Leathart JB, Swainsbury RA, Dang TS, Day CP (2007) Genetic susceptibility to diclofenac-induced hepatotoxicity: contribution of UGT2B7, CYP2C8, and ABCC2 genotypes. *Gastroenterology* 132:272281
- de Abajo FJ, Montero D, Madurga M, García Rodríguez LA (2004) Acute and clinically relevant drug-induced liver injury: a population based case–control study. *Br J Clin Pharmacol* 58:71–80
- Degen PH, Dieterle W, Schneider W, Theobald W, Sinterhauf U (1988) Pharmacokinetics of diclofenac and five metabolites after single doses in healthy volunteers and after repeated doses in patients. *Xenobiotica* 18:144955
- Dickie AP, Wilson CE, Schreiter K, Wehr R, Wilson EM, Bial J, Scheer D, Wilson ID, Riley RJ (2017) The pharmacokinetics and metabolism of lumiracoxib in chimeric humanized and murinized FRG mice. *Biochem Pharmacol* 135:139–150
- Faigle JW, Böttcher I, Godbillon J, Kriemler HP, Schlumpf E, Schneider W, Schweizer A, Stierlin H, Winkler T (1988) A new metabolite of diclofenac sodium in human plasma. *Xenobiotica* 18:1191–1197
- Gomez-Lechon MJ, Ponsoda X, O'Connor E, Donato T, Castell JV (2003a) Diclofenac induces apoptosis in hepatocytes. *Toxicol In Vitro* 17:675680
- Gomez-Lechon MJ, Ponsoda X, O'Connor E, Donato T, Castell JV, Jover R (2003b) Diclofenac induces apoptosis in hepatocytes by alteration of mitochondrial function and generation of ROS. *Biochem Pharmacol* 66:21552167
- Hammond TG, Meng X, Jenkins RE, Maggs JL, Castelazo AS, Regan SL, Bennett SNL, Earnshaw CJ, Aithal GP, Pande I, Kenna JG, Stachulski AV, Park BK, Williams DP (2014) Mass spectrometric characterization of circulating covalent protein adducts derived from a drug acyl glucuronide metabolite: multiple albumin adductions in diclofenac patients. *J Pharmacol Exp Ther* 350:387402
- Hargus SJ, Amouzedeh HR, Pumford NR, Myers TG, McCoy SC, Pohl LR (1994) Metabolic activation and immunochemical localization of liver protein adducts of the nonsteroidal anti-inflammatory drug diclofenac. *Chem Res Toxicol* 7:575582
- Kamimura H, Nakada N, Suzuki K, Mera A, Souda K, Murakami Y, Tanaka K, Iwatsubo T, Kawamura A, Usui T (2010) Assessment of chimeric mice with humanized liver as a tool for predicting circulating human metabolites. *Drug Metab Pharmacokin* 25:223235
- Kola I, Lanhis J (2004) Can the pharmaceutical industry reduce attrition rates? *Nat Rev Drug Discovery* 3:711716
- Kretz-Rommel A, Boelsterli U (1993) Diclofenac covalent protein binding is dependent on acyl glucuronide formation and is inversely related to acute cell injury in cultured rat hepatocytes. *Toxicol Appl Pharmacol* 120:155161
- Kretz-Rommel A, Boelsterli UA (1994) Selective protein adducts to membrane proteins in cultured rat hepatocytes exposed to diclofenac. Radiochemical and immunochemical analysis. *Mol Pharmacol* 45:237244
- Kumar S, Samuel K, Subramanian R, Braun MP, Stearns RA, Chiu SH, Evans DC, Baillie TA (2002) Extrapolation of diclofenac clearance from in vitro microsomal metabolism data: role of acyl glucuronidation and sequential oxidative metabolism of the acyl glucuronide. *J Pharmacol Exp Ther* 303:96978
- Le HT, Franklin MR (1997) Selective induction of phase II drug metabolizing enzyme activities by quinolines and isoquinolines. *Chem Biol Interact* 103:167178
- Lichtenstein D, Sygal S, Wolfe M (1995) Nonsteroidal antiinflammatory drugs and the gastrointestinal tract: the double-edged sword. *Arthritis Rheum* 38:518
- Lim MS, Lim PLK, Gupta R, Boelsterli UA (2006) Critical role of free cytosolic calcium, but not uncoupling, in mitochondrial permeability transition and cell death induced by diclofenac oxidative metabolites in immortalized human hepatocytes. *Toxicol Appl Pharmacol* 217:322331
- LoGuidice A, Wallace BA, Bendel L, Redinbo MR, Boelsterli UA (2012) Pharmacologic targeting of bacterial B-glucuronidase alleviates nonsteroidal anti-inflammatory drug-induced enteropathy in mice. *J Pharmacol Exp Therapeutics* 341:447–454
- Martinez C, Garcia-Martin E, Ladero JM, Herraes O, Ortega L, Taxonera C, Suárez A, DíazRubio M, Agúndez JA (2007) GSTT1 and GSTM1 null genotypes may facilitate hepatitis C virus infection becoming chronic. *J Infect Dis* 195:13201323
- Masubuchi Y, Nakayama S, Horie T (2002) Role of mitochondrial permeability transition in diclofenac-induced hepatocyte injury in rats. *Hepatology* 35:544551
- Park BK, Coleman JW, Kitteringham NR (1987) Drug disposition and drug hypersensitivity. *Biochem Pharmacol* 36:58190

- Petrescu I, Tarba C (1997) Uncoupling effects of diclofenac and aspirin in the perfused liver and isolated hepatic mitochondria of rat. *Biochim Biophys Acta* 1318:38594
- Pickup K, Gavin A, Jones HB, Karlsson E, Page C, Ratcliffe K, Sarda S, Schulz-Utermoehl T, Wilson I (2012) The hepatic reductase null mouse as a model for exploring hepatic conjugation of xenobiotics: application to the metabolism of diclofenac. *Xenobiotica* 42:195–205
- Poon GK, Chen Q, Teffera Y, Ngui JS, Griffin PR, Braun MP, Doss GA, Freedden C, Stearns RA, Evans DC, Baillie TA, Tang W (2001) Bioactivation of diclofenac via benzoquinone imine intermediates-identification of urinary mercapturic acid derivatives in rats and humans. *Drug Metab Dispos* 29:1608–1613
- Reid G, Wielinga P, Zelcer N, De Haas M, Van Deemter L, Wijnholds J, Balzarini J, Borst P (2003) Characterization of the transport of nucleoside analog drugs by the human multidrug resistance proteins MRP4 and MRP5. *Mol Pharmacol* 63:1094103
- Riess W, Stierlin H, Degen P, Faigle JW, Gérardin A, Moppert J, Sallmann A, Schmid K, Schweizer A, Sulc M, Theobald W, Wagner J (1978) Pharmacokinetics and metabolism of the antiinflammatory agent Voltaren. *Scand J Rheumatol Suppl* 22:17–29
- Sarda S, Page C, Pickup K, Schulz-Utermoehl T, Wilson I (2012) Diclofenac metabolism in the mouse: novel in vivo metabolites identified by high performance liquid chromatography coupled to linear ion trap mass spectrometry. *Xenobiotica* 42:179194
- Sarda S, Partridge EA, Pickup K, McCarthy A, Wilson I (2014) HPL-CMS profiling and structural identification of [¹⁴C]-diclofenac metabolites in mouse bile. *Chromatographia* 77:233239
- Scheer N, Wilson ID (2016) A comparison between genetically humanized and chimeric liver humanized mouse models for studies in drug metabolism and toxicity. *Drug Discov Today* 21:250263
- Schmeltzer PA, Kosinski AS, Kleiner DE, Hoofnagle JH, Stolz A, Fontana RJ, Russo MW (2016) Liver injury from nonsteroidal anti-inflammatory drugs in the United States. *Liver Int* 36:603609
- Schneider HT, Nuernberg B, Dietzel K, Brune K (1990) Biliary elimination of non-steroidal antiinflammatory drugs in patients. *Br J Clin Pharmacol* 29:127–31
- Scialis RJ, Manautou JE (2016) Elucidation of the mechanisms through which the reactive metabolite diclofenac acyl glucuronide can mediate toxicity. *J Pharmacol Exp Ther* 57:167–76
- Shaw PJ, Ganey PE, Roth RA (2010) Idiosyncratic drug-induced liver injury and the role of inflammatory stress with an emphasis on an animal model of trovafloxacin hepatotoxicity. *Toxicol Sci* 118:718
- Stierlin H, Faigle JW (1979) Biotransformation of diclofenac sodium (Voltaren) in animals and in man. II. Quantitative determination of the unchanged drug and principal phenolic metabolites, in urine and bile. *Xenobiotica* 9:611–21
- Stierlin H, Faigle JW, Sallmann A, Küng W, Richter WJ, Kriemler HP, Alt KO, Winkler T (1979) Biotransformation of diclofenac sodium (Voltaren) in animals and in man. I. Isolation and identification of principal metabolites. *Xenobiotica* 9:601–10
- Strom SC, Davila J, Grompe M (2010) Chimeric mice with humanized liver: tools for the study of drug metabolism, excretion, and toxicity. *Methods Mol Biol* 640:491509
- Tang W, Stearns RA, Bandiera SM, Zhang Y, Raab C, Braun MP, Dean DC, Pang J, Leung KH, Doss GA, Strauss JR, Kwei GY, Rushmore TH, Chiu SH, Baillie TA (1999) Studies on cytochrome P-450-mediated bioactivation of diclofenac in rats and in human hepatocytes: identification of glutathione conjugated metabolites. *Drug Metab Dispos* 27:365372
- Uetrecht J (2003) Screening for the potential of a drug candidate to cause idiosyncratic drug reactions. *Drug Discov Today* 8:832–837
- Waring MJ, Arrowsmith J, Leach AR, Leeson PD, Mandrell S, Owen RM, Pairaudeau G, Pennie WD, Pickett SD, Wang J, Wallace O, Weir A (2015) An analysis of the attrition of drug candidates from four major pharmaceutical companies. *Nat Rev Drug Discov* 14:475486
- Willis JV, Kendall MJ, Flinn RM, Thornhill DP, Welling PG (1976) The pharmacokinetics of diclofenac sodium following intravenous and oral administration. *Eur J Clin Pharmacol* 16:405410
- Zhang Y, Han YH, Putluru SP, Matta MK, Kole P, Mandlekar S, Furlong MT, Liu T, Iyer RA, Marathe P, Yang Z, Lai Y, Rodrigues AD (2016) Diclofenac and its acyl glucuronide: determination of in vivo exposure in human subjects and characterization as human drug transporter substrates in vitro. *Drug Metab Dispos* 44:320328
- Zhou SF, Zhou ZW, Yang LP, Cai JP (2009) Substrates, inducers, inhibitors and structure-activity relationships of human cytochrome P450 2C9 and implications in drug development. *Curr Med Chem* 16:34803675